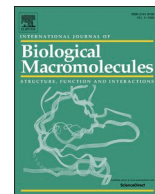




Since January 2020 Elsevier has created a COVID-19 resource centre with free information in English and Mandarin on the novel coronavirus COVID-19. The COVID-19 resource centre is hosted on Elsevier Connect, the company's public news and information website.

Elsevier hereby grants permission to make all its COVID-19-related research that is available on the COVID-19 resource centre - including this research content - immediately available in PubMed Central and other publicly funded repositories, such as the WHO COVID database with rights for unrestricted research re-use and analyses in any form or by any means with acknowledgement of the original source. These permissions are granted for free by Elsevier for as long as the COVID-19 resource centre remains active.



## Mucosal IgA response elicited by intranasal immunization of *Lactobacillus plantarum* expressing surface-displayed RBD protein of SARS-CoV-2

Letian Li<sup>a,1</sup>, Maopeng Wang<sup>b,1</sup>, Jiayi Hao<sup>a,c,1</sup>, Jicheng Han<sup>d</sup>, Tingting Fu<sup>a</sup>, Jieying Bai<sup>e</sup>, Mingyao Tian<sup>a</sup>, Ningyi Jin<sup>a,d</sup>, Guangze Zhu<sup>d,\*</sup>, Chang Li<sup>a,\*</sup>

<sup>a</sup> Research Unit of Key Technologies for Prevention and Control of Virus Zoonoses, Chinese Academy of Medical Sciences, Changchun Institute of Veterinary Medicine, Chinese Academy of Agricultural Sciences, Changchun 130122, China

<sup>b</sup> Institute of Virology, Wenzhou University, Wenzhou 325035, China

<sup>c</sup> College of Veterinary Medicine, Jilin Agricultural University, Changchun 130118, China

<sup>d</sup> Academician Workstation of Jilin Province, Changchun University of Chinese Medicine, Changchun 130021, China

<sup>e</sup> Institute of Molecular Medicine, Peking University, Beijing 100871, China

### ARTICLE INFO

#### Keywords:

*Lactobacillus plantarum*

SARS-CoV-2

Receptor-binding domain (RBD)

Mucosal vaccine

Intranasal immunization

### ABSTRACT

Coronavirus Disease 2019 (COVID-19) caused by a novel betacoronavirus SARS-CoV-2 has been an ongoing global pandemic. Several vaccines have been developed to control the COVID-19, but the potential effectiveness of the mucosal vaccine remains to be documented. In this study, we constructed a recombinant *L. plantarum* LP18:RBD expressing the receptor-binding domain (RBD) of the SARS-CoV-2 spike protein via the surface anchoring route. The amount of the RBD protein was maximally expressed under the culture condition with 200 ng/mL of inducer at 33 °C for 6 h. Further, we evaluated the immune response in mice via the intranasal administration of LP18:RBD. The results showed that the LP18:RBD significantly elicited RBD-specific mucosal IgA antibodies in respiratory tract and intestinal tract. The percentages of CD3 + CD4+ T cells in spleens of mice administrated with the LP18:RBD were also significantly increased. This indicated that LP18:RBD could induce a humoral immune response at the mucosa, and it could be used as a mucosal vaccine candidate against the SARS-CoV-2 infection. We provided the first experimental evidence that the recombinant *L. plantarum* LP18:RBD could initiate immune response in vivo, which implies that the mucosal immunization using recombinant LAB system could be a promising vaccination strategy to prevent the COVID-19 pandemic.

### 1. Introduction

Since December 2019, the novel infectious disease named Corona Virus Disease 2019 (COVID-19) has been an ongoing pandemic and threatening the life of all human beings. Severe Acute Respiratory Syndrome Coronavirus 2 (SARS-CoV-2), the etiological agent of COVID-19, is similar to the SARS-CoV and causes the severe respiratory syndrome. As a new member of betacoronavirus, SARS-CoV-2 shows very high transmissibility among people [1]. Its spike (S) protein that is consisted of 1273 amino acids, has been focused on as the main antigen target for developing vaccines or antibodies. Spikes are displayed on the surface of the virus and assists in viral attachment and entrance to the host cells by interacting with the receptor angiotensin-converting enzyme 2 (ACE2) [2]. There are highly conserved epitopes in the

receptor-binding domain (RBD) of the spike protein between SARS-CoV-2 and SARS-CoV, and the RBD of SARS-CoV-2 is also the major target for neutralizing antibodies [3,4]. Several vaccines targeting spike protein, such as inactivated vaccine, subunit vaccine, DNA vaccine, mRNA-based vaccine, and virus-vector-based vaccine have been developed or approved for controlling COVID-19 [5–7]. However, there are still some limitations in the development of vaccines, such as relevant to production capacity, cold-chain transportation, specific devices required, and adverse reaction of injection, which challenge the use of the vaccine in underdeveloped countries [8]. Therefore, mucosal vaccines are more attractive because of their advantages in directly targeting infections' sites, activation of local and systemic immune responses, and convenience for transportation or administration [9].

*Lactobacillus plantarum* (*L. plantarum*) has been considered as a safe

\* Corresponding authors.

E-mail addresses: [zhuguangze820@126.com](mailto:zhuguangze820@126.com) (G. Zhu), [lichang78@163.com](mailto:lichang78@163.com) (C. Li).

<sup>1</sup> These authors contributed equally to this work.

and stable delivery carrier for mucosal vaccines. Recently, some recombinant *L. plantarum* strains for vaccine delivery have been constructed and the good immunogenicity has been validated in oral or nasal immunization [10]. Above all, the antigens displaying on the surface of *L. plantarum* can initiate a prominent immune response [11–13]. This study aimed to utilize a food-grade *L. plantarum* CGMCC 1.557 (also named LP18) by constructing a recombinant *L. plantarum* expressing SARS-CoV-2 RBD on its surface. Further, this study planned to verify the immunogenicity of recombinant *L. plantarum* using a mice model adopting intranasal immunization.

## 2. Materials and methods

### 2.1. Bacterial strains, plasmid, and animals

The *Lactococcus lactis* strain NZ3900, *Lactobacillus plantarum* CGMCC 1.557 (LP18) strain, and plasmid pSIP411 [14] were obtained or cultured as previously reported [15].

Six-weeks-old female BALB/c mice (SPF Biotechnology, China) were housed under pathogen-free standard environmental conditions (12 h light/dark cycle and 22 °C–25 °C, 45%–50% relative humidity) and provided with standard food and water ad libitum. The animal experimental procedures were approved by the Laboratory Animal Welfare and Ethics Committee of the Academy of Military Medical Sciences (approval ID: IACUC of AMMS-11-2020-006).

### 2.2. Construction of recombinant *L. plantarum*

The sequence *1320-tSDH* was obtained from the previous study [16], which consisted of a codon-optimized spike gene derived from the SARS-CoV-2 isolate Wuhan-Hu-1 (GenBank: MN908947). In the sequence *1320-tSDH*, as shown in Fig. 1A, a sequence of the endogenous signal peptide 1320 (GenBank: CP016270.1, locus tag: ALX04\_001320) derived from *L. plantarum* was linked to the 5' terminus of spike gene, a dendritic cell (DC)-targeting peptide, DCpep (peptide: FYPSTHSTPQRP) [17] and hemagglutinin (HA)-epitope tag (peptide: YPYDVPDYA) was linked to the 3' terminus of spike gene. To obtain the recombinant plasmid containing the sequence of RBD, as shown in Fig. 1A–B, two steps PCR was performed to generate a fragment *1320-RBDDH*, subsequently, the fragment *1320-RBDDH* was subcloned into the plasmid pSIP411. The primers in this study are shown in Table 1. Afterward, the recombinant plasmid pLP-RBD was immediately electrotransformed successively into competent *L. lactis* NZ3900 and *L. plantarum* LP18 cells as described previously [15]. The positive colony was screened out on a GM17 (Hopebiol, China) or MRS (Hopebiol, China) agar plate containing 10 µg/mL erythromycin (Sigma-Aldrich, USA), and further verified by PCR using the primers 411-test-F and 411-test-R. The verified positive colony of recombinant *L. plantarum* was designated as LP18:RBD. Likewise, an *L. plantarum* LP18 strain harboring original pSIP411 (empty vector) was constructed and designated as LP18:vector.

### 2.3. Identification of recombinant RBD (rRBD) protein expressed by LP18:RBD

The LP18:RBD were cultured overnight in advance, and 100 µL of culture was added into 10 mL of MRS broth containing 10 µg/mL erythromycin. When the OD600 of the broth reaches 0.3–0.5, the inducer SppIP [18] (GenScript Biotech, China) was added into the culture at a concentration of 50 ng/mL. The LP18:RBD was incubated at 37 °C for 8 h. Subsequently, the LP18:RBD cells were harvested, washed twice with PBS, and crushed with 0.1 µm glass beads (Sigma-Aldrich, USA) for 20 min. The bacterial protein in the lysates, was mixed with 5 × loading buffer and boiled in a water bath for complete denaturation. The bacterial protein was evaluated by western blotting. Briefly, the protein samples were separated by 10% SDS-PAGE gel and electrotransferred onto a PVDF membrane (Millipore, USA). The membrane

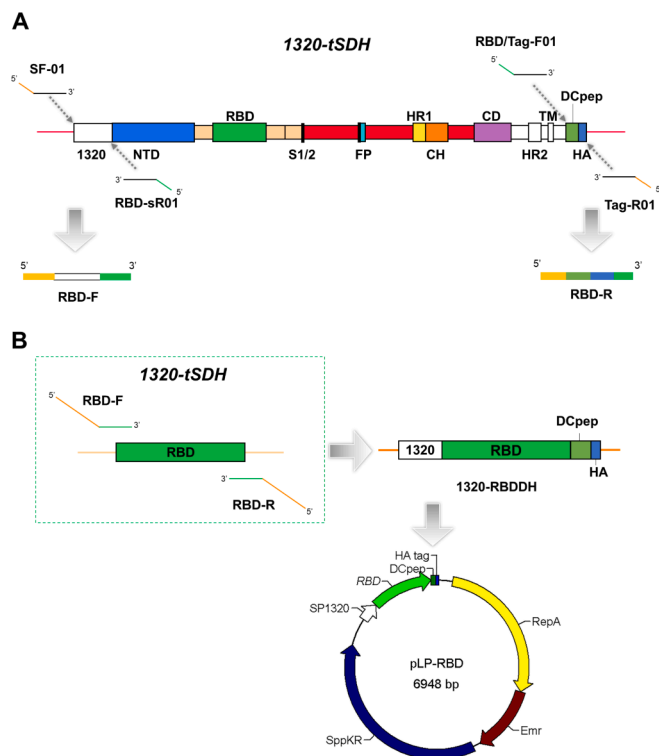


**Fig. 1.** The schematic diagram of the recombinant plasmid pLP-RBD. (A) Schematic diagram of the sequence *1320-tSDH*. 1320, signal peptide 1320; NTD, N-terminus domain; RBD, receptor-binding domain; FP, fusion peptide; HR1, heptad repeat 1; CH, central helix; CD, connector domain; HR2, heptad repeat 2; TM, transmembrane domain; DCpep, DC-targeting peptide; HA, HA-epitope tag. The fragments *RBD-F* (281 bp in the signal peptide 1320) and *RBD-R* (113 bp in the DCpep and HA tag) were amplified from *1320-tSDH* by PCR with primers, SF-01, RBD-sR01, and RBD/Tag-F01, Tag-R01 respectively. (B) Fragments *RBD-F* and *RBD-R* were used as primers targeting the RBD sequence in *1320-tSDH*, and extension-PCR was performed to obtain the fragment *1320-RBDDH* (1132 bp), which consists of signal peptide 1320, sequence of RBD, DCpep, and HA tag in order from 5' to 3'. Subsequently, fragment *1320-RBDDH* was subcloned into the plasmid pSIP411 by using the Clone Express Multis One Step Cloning Kit (Vazyme Biotech, China), giving rise to recombinant plasmid pLP-RBD.

was blocked by 5% skim milk solution at room temperature for 2 h, followed by incubating with anti-HA tag rabbit polyclonal antibody (1:1000, Proteintech, USA) or anti-RBD mouse monoclonal antibody 13E10D5 (1:1000, GenScript Biotech, China) at 4 °C overnight and washed with TBST four times. Thereafter, the membrane was incubated with horseradish peroxidase (HRP)-conjugated secondary antibody (1:10000, Beyotime Biotechnology, China) at room temperature for 1 h, and washed with TBST four times. Subsequently, the proteins were visualized using enhanced chemiluminescence (ECL) reagent (Thermo Fisher Scientific, USA) in GE Amersham Imager600.

On the other hand, the rRBD protein displayed on bacteria, was identified by indirect immunofluorescence assay (IFA) and flow cytometric analysis (FCM). As in the previous study [16], the induced LP18:RBD, LP18:vector, and LP18 cells were harvested and washed twice with PBS. The cells were then resuspended and incubated with anti-HA tag rabbit polyclonal antibody (1:100) at 4 °C overnight. After washing three times with PBS, the cells were incubated with an FITC-conjugated goat anti-rabbit IgG (1:5000, Beyotime Biotechnology) at room temperature for 40 min and washed again. An aliquot of suspended cells was fixed on a clean coverslip in the dark and imaged using a fluorescence microscope (ZEISS, Japan). Extra suspended cells were examined using a CytoFLEX flow cytometer (Beckman Coulter, USA) by FITC tunnel assay.

**Table 1**  
Primers used in this study.

Primers	Sequence (5'-3')	Production size (bp)
SF-01	TATTACAAGGAGATTTTAGCCATGGAGATTTTAGCCATG	281
RBD-sR01	<u>GGGCACAAGTTCGTAATATTG</u> <sup>a</sup> GGTTCTTACCAGACGGTATAAC	
RBD/Tag-F01	<u>CGCACGTAGTGTGCTAGTCAA</u> <sup>b</sup> TTTTATCCGAGTTATCATAGTACGCC	113
Tag-R01	GGGGTACCGAATTCCTCGA	
411-test-F	GCTTCCACACGCATTTCAG	1760
411-test-R	ATTCTGCTCCGCCCTTATG	

<sup>a</sup> The homologous sequence from 5' terminus of RBD.

<sup>b</sup> The homologous sequence from 3' terminus of RBD.

#### 2.4. Optimization of expression

To optimize the dosage of the inducer, the LP18:RBD was induced with 25, 50, 100, 150, and 200 ng/mL of SppIP, respectively at 37 °C for 8 h. Then bacterial protein samples were prepared as described above and homogenized samples were quantified using BCA protein assay kit (Beyotime Biotechnology, China). The expression level of rRBD protein in samples was evaluated by western blotting. For optimization of induction time, the LP18:RBD was induced with 100 ng/mL of SppIP at 37 °C for 4, 6, 8, 10, 12, 16, 20, and 24 h, respectively. For optimization of temperature, the LP18:RBD was induced with 100 ng/mL of SppIP for 6 h at 33 °C, 37 °C, and 42 °C, respectively. Similarly, the expression level of rRBD protein was evaluated as described above.

#### 2.5. Semi-quantitative western blotting

To estimate the yield of rRBD protein expressed in the LP18:RBD, the semi-quantitative western blotting as described elsewhere was performed [19,20]. Briefly, the samples of total protein were obtained from the induced LP18:RBD, and the concentration of total protein was measured by BCA assay. Subsequently, the rRBD protein in the sample was evaluated by western blotting with anti-RBD mouse monoclonal antibody 13E10D5 using as primary antibody (1:1000). The RBD protein expressed by the Chinese hamster ovary (CHO) cell (GenScript Biotech, China) was utilized as standard at 31.25 ng, 62.5 ng, 125 ng, 250 ng, and 500 ng amounts. The standard curve and regression equation were established by designating the gray value of standard RBD protein as X-axis, and the mass of RBD protein as Y-axis. The yield of rRBD protein was calculated according to the regression eq.

#### 2.6. Immunization

A total of 36 BALB/c mice were randomly divided into three groups, PBS group (n = 12), LP18 group (n = 12), and LP18:RBD group (n = 12), respectively. The procedure of immunization is shown in Fig. 2. The LP18:RBD or LP18 cells were prepared under optimized conditions, then the bacterial pellets were suspended in sterile PBS, and the suspension was given intranasally to anesthetized mice. Every mouse was administered 20  $\mu$ L of PBS (negative control) or PBS containing  $1 \times 10^9$  CFU of LP18 or LP18:RBD for three consecutive days (days 1, 2, and 3), and booster immunizations were administered with the same way at 14 days later (days 15, 16, and 17). Three batches of mice were sacrificed by cervical dislocation under anesthesia at days 14, 21, and 56 for collecting samples.

#### 2.7. Sample collection

Nasal lavage fluid (NLF) samples were collected from individual mice, postmortem. A pipettor was used to flush the nasal cavity with 10  $\mu$ L of PBS containing 1% bovine serum albumin (BSA, Sigma-Aldrich, USA) and 1 mM phenylmethanesulfonyl fluoride (PMSF, Beyotime Biotechnology, China), the process was repeated 6 times, and the lavage fluid was recovered as much as possible. The NLF samples were tested immediately or stored at  $-20$  °C until use.

Bronchoalveolar lavage fluid (BALF) samples were collected from the individual mice, postmortem. After exposing the trachea, a feeding needle was inserted into the exposed trachea and kept in place. A syringe was attached to inject and withdraw 500  $\mu$ L of PBS containing 1% BSA and 1 mM PMSF three times. The BALF samples were placed on ice before centrifugation at  $3000 \times g$ , 4 °C for 10 min, the supernatants were collected for testing immediately or stored at  $-20$  °C until use.

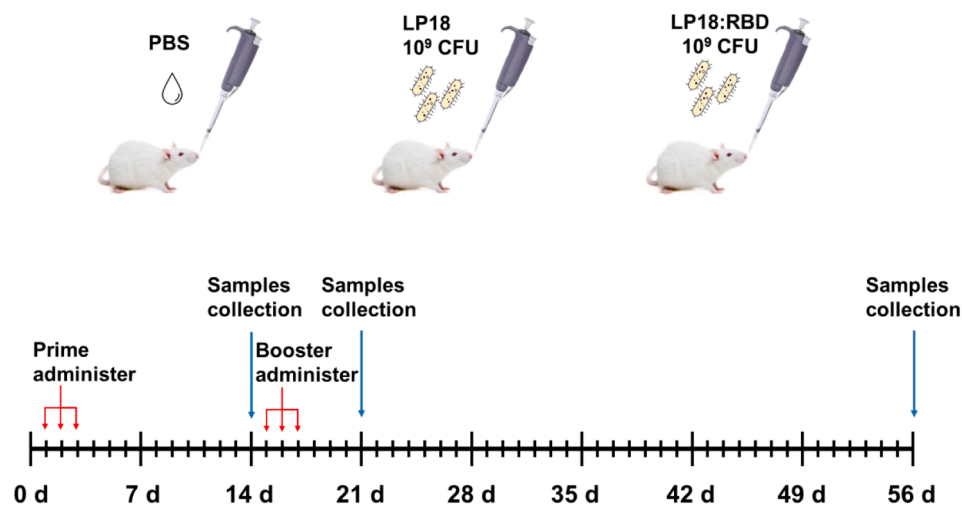


**Fig. 2.** Groups and schedule for immunization. Three groups of mice were administered PBS,  $1 \times 10^9$  CFU of LP18:RBD, or LP18, respectively via the intranasal route. The prime immunization was administered at days 1, 2, and 3, and the boost immunization was administered at days 15, 16, and 17. Samples were collected on days 14, 21, and 56.

Fecal samples were collected and pooled from all mice in each group. Fresh fecal pellets resuspended with PBS containing 1% BSA and 1 mM PMSF to a concentration of 100 mg/mL. After homogenization by vortex and incubation at 4 °C overnight, fecal samples were centrifuged at 10,000 ×g for 10 min. The supernatants were collected for testing immediately or stored at –20 °C until use.

## 2.8. Indirect ELISA for detecting IgA antibodies

The SARS-CoV-2 mouse IgG indirect ELISA kit (DaRui biotech, China) was utilized with modifications to detect antigen-specific IgA antibodies in the BALF, NLF, and fecal samples. Briefly, the samples were diluted with PBS before testing. The BALF samples were tested without dilution, the NLF and fecal samples were diluted with PBS (1:5), 100 µL of diluted samples were added into every well of microtiter plate precoated with RBD protein of SARS-CoV-2, and the plate was incubated at 37 °C for 60 min. After the plate was washed using PBST, HRP-conjugated goat anti-mouse IgA (1:20000, Abcam, USA) was added into the wells, and the plate was incubated at 37 °C for 20 min. The plate was washed again and visualized using tetramethylbenzidine (TMB) in the dark for 10 min. Finally, the reaction was stopped with 2 M sulfuric acid solution. The absorbance was measured at 450 nm with the reference wavelength set to 630 nm by microplate reader (Tecan, Switzerland).

## 2.9. Detection of CD3 + CD4+ and CD3 + CD8+ T cells in splenic lymphocytes

The splenic lymphocytes of mice were isolated using a splenic lymphocytes isolation kit (TBD science, China). Briefly, the splenocytes were isolated from fresh spleen by gentle crushing in DMEM (HyClone, USA). After filtering through the 70 µm screen, the suspension was transferred slowly onto an isolation reagent. After horizontal centrifugation for 30 min, the lymphocytes were collected from the interlayer. Subsequently, the lymphocytes were washed and resuspended in the sterile PBS, and  $1 \times 10^6$  lymphocytes were stained with APC anti-mouse CD3, FITC anti-mouse CD4, and PE anti-mouse CD8 antibodies (BioLegend, USA) in the dark for 40 min. After washing, the proportion of CD3 + CD4+ or CD3 + CD8+ T cells from the stained lymphocytes were analyzed using the FCM.

## 2.10. Statistical tests

Statistical significance was determined by one-way analyses of variance (ANOVAs) with Tukey tests using GraphPad Prism (GraphPad Software, USA). Results are presented as means ± SEM. Statistical significance is shown as follows: \*p < 0.05; \*\*p < 0.01.

## 3. Results

### 3.1. Construction of recombinant *L. plantarum* expressing SARS-CoV-2 RBD protein

The fragment *RBD-F* (281 bp) containing 1320 signal peptide and 26 bp homologous sequence at 5' of *RBD* was firstly obtained by PCR. Likewise, the fragment *RBD-R* (113 bp) containing 26 bp homologous sequence at 3' of *RBD*, target peptide D (DCpep), and HA-tag was obtained (Fig. 3A). Then an overlap extension-PCR was performed to obtain the target sequence *1320RBDH* (1132 bp) from pUC57-1320-tSDH (Fig. 3B). The *1320RBDH* was combined with the linearized pSIP411 (Fig. 3C) to give rise to a recombinant plasmid. The recombinant *L. plantarum* LP18:RBD was verified based on the 1760 bp product from the colony PCR (Fig. 3D).

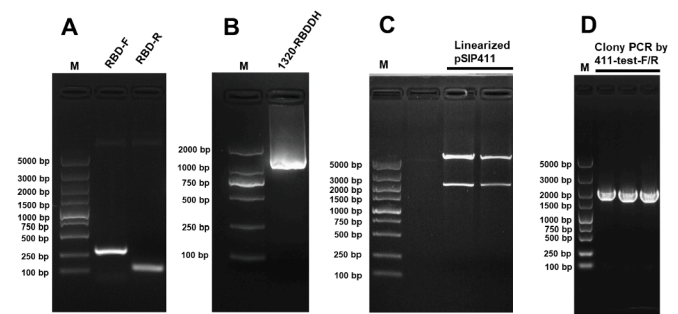


**Fig. 3.** Recombinant SARS-CoV-2 RBD sequence was cloned into *L. plantarum* strain LP18. (A) The 281 bp fragment *RBD-F* and the 113 bp fragment *RBD-R* were amplified by PCR. (B) The 1132 bp fragment *1320-RBDH* was obtained by overlap extension-PCR. (C) The linearized plasmid pSIP411 was obtained by double digestion with *Nco* I and *Xho* I, and the digested product was 5855 bp. (D) The positive colonies from the screening plate were verified by PCR using the primers 411-test-F and 411-test-R, showing 1760 bp fragments.

### 3.2. Identification of rRBD protein expressed on LP18:RBD

The LP18:RBD were incubated with the SppIP at 37 °C for 8 h, and the cells were harvested and crushed in PBS. The rRBD protein from the supernatant was detected by western blotting. As a result, about 40 kDa band of rRBD protein was detected using anti-HA tag rabbit polyclonal antibody and anti-RBD mouse monoclonal antibody 13E10D5 as the primary antibody (Fig. 4A), which demonstrated that rRBD protein has been expressed by the LP18:RBD effectively and recognized using specific antibodies.

To identify that rRBD protein has been displayed on the cell surface, the induced LP18:RBD was examined using IFA and FCM. The results showed that the rRBD proteins on the surface of cells has been captured by fluorophore-labeled antibody (Fig. 4B). In FCM, the LP18:RBD showed a shifted positive peak, and the positive rate of the detected rRBD was 31.79% compared with the LP18:vector used as negative control (Fig. 4C). These results suggested that the RBD protein could be efficiently displayed on the surface of the LP18:RBD cells.

### 3.3. Optimizing and evaluating the expression level of rRBD protein

The expression level of recombinant protein in recombinant *L. plantarum* could be affected by the dosage of inducer, time of induction, and temperature of incubation [16]. Therefore, these conditions were investigated for the maximization of expression. As shown in Fig. 5A–C, the best expression level of rRBD protein was obtained with 200 ng/mL of SppIP at 33 °C for 6 h. Furthermore, the yield of the rRBD protein from one dose of the bacterial vaccine was measured by semi-quantitative western blotting. The 250 µL of total proteins were obtained from  $10^9$  CFU (by colony-counting methods) of the induced LP18:RBD, and its concentration was shown to be 4.22 mg/mL by BCA assay. Subsequently, the rRBD protein in the 16 µL of total protein was evaluated by western blotting with the simultaneous use of standard RBD proteins as reference. According to the standard curve and regression equation generated from standard RBD proteins, as shown in Fig. 5D, the 203.9 ng of rRBD protein was calculated in the 67.5 µg of total proteins. Therefore, the quantity of rRBD protein in  $10^9$  CFU (250 µL with the concentration of 4.22 mg/mL total proteins) of the LP18:RBD cells was approximately 3.17 µg. The yield of rRBD protein was measured as 0.3% (203.9 ng rRBD protein in 67.5 µg total protein).

### 3.4. Antigen-specific IgA antibody responses elicited by LP18:RBD in mice

To investigate the activation of humoral immunity stimulated by the LP18:RBD in mice, the antigen-specific IgA antibody in BALF, NLF, and fecal samples were detected on the 14, 21, and 56 days after prime



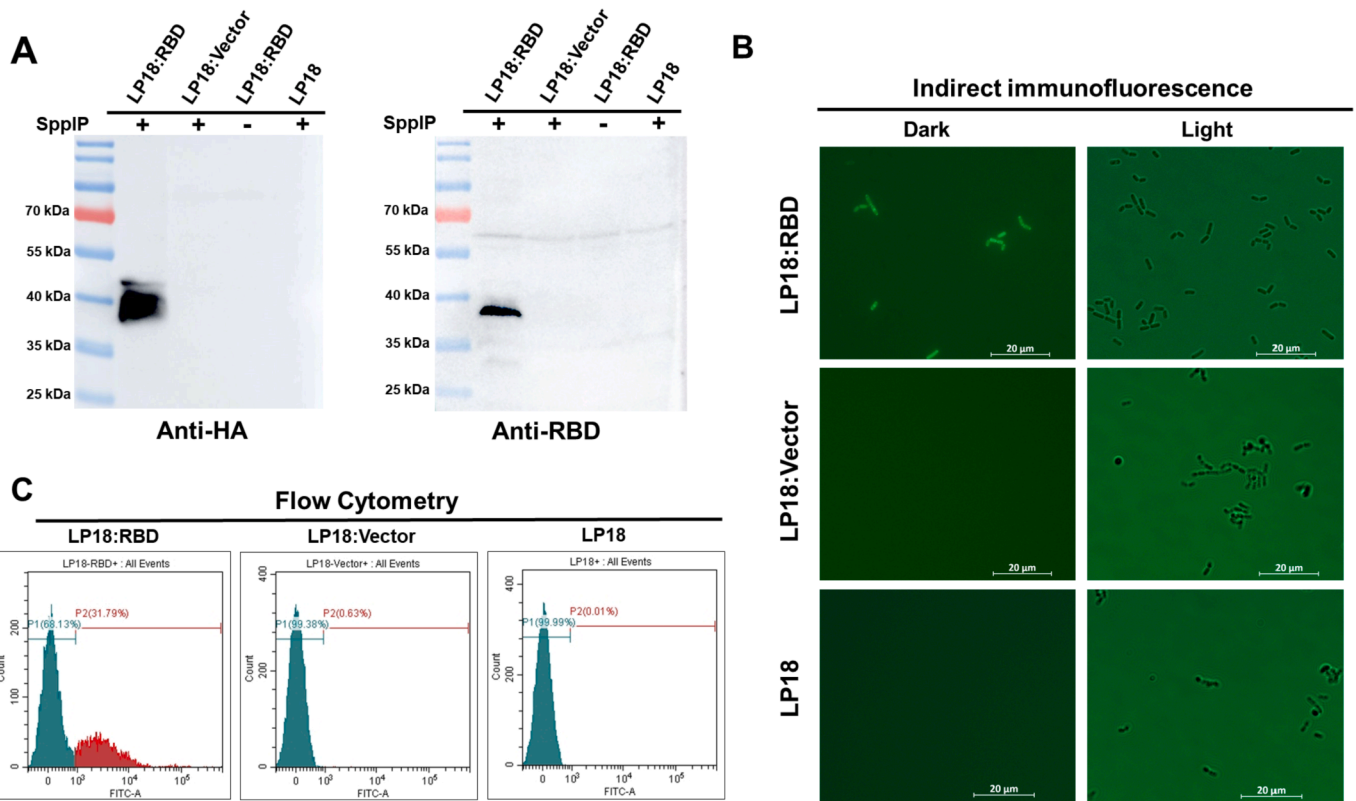


**Fig. 4.** Identification of LP18:RBD expressing SARS-CoV-2 RBD protein. (A) The rRBD protein expressed in the induced LP18:RBD was detected by western blotting using anti-HA tag rabbit polyclonal antibody (left panel), and anti-RBD mouse monoclonal antibody 13E10D5 (right panel) as the primary antibody. The samples from the LP18:RBD without induction, induced LP18:vector, and LP18 were detected as control. (B) Indirect immunofluorescence assay was performed using anti-HA tag rabbit polyclonal antibody as primary antibody and a FITC-conjugated secondary antibody to verify if the rRBD protein has been expressed on the surface of the LP18:RBD. The induced LP18:vector and LP18 were detected as controls, which were imaged under a 100× objective lens of a fluorescence microscope using the excitation wavelength of 488 nm and emission wavelength of 590 nm. (C) The LP18:RBD displaying rRBD protein was evaluated by FCM. The induced LP18:vector and LP18 were detected as control.

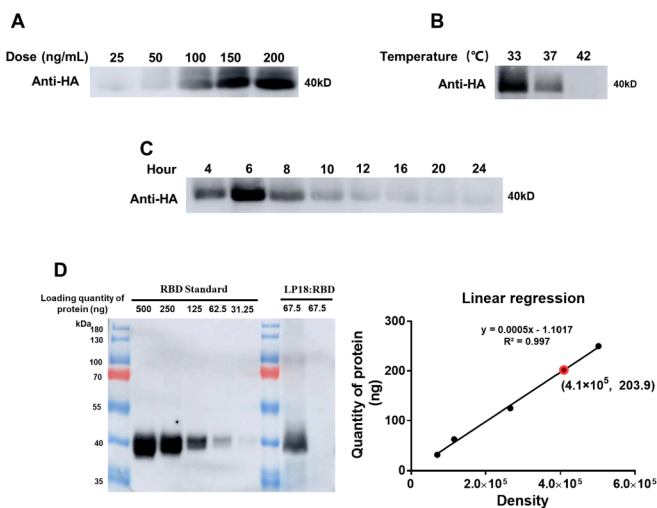


**Fig. 5.** Optimization of culture conditions for the LP18:RBD and evaluation of the expression level of rRBD protein. The LP18:RBD cells were cultured and induced by different SppIP concentrations (A), various incubation temperatures (B), and different induction times (C), subsequently, the expression of rRBD protein was evaluated by western blotting. (D) Semi-quantitative western blotting was performed to assess the expression yield of rRBD protein, which was calculated by a regression curve from a series of standard RBD proteins.

immunization. The results showed that the IgA in BALF samples of the LP18:RBD group was significantly increased, compared with the PBS or LP18 group from 14 days ( $p < 0.05$  or  $p < 0.01$ , Fig. 6A). Similarly, the IgA in NLF samples of the LP18:RBD group was significantly increased from 21 days ( $p < 0.01$ , Fig. 6B). The IgA in both of BALF and NLF samples of the LP18:RBD group maintained a higher level until 56 days. Notably, the IgA in fecal samples of LP18:RBD group was significantly

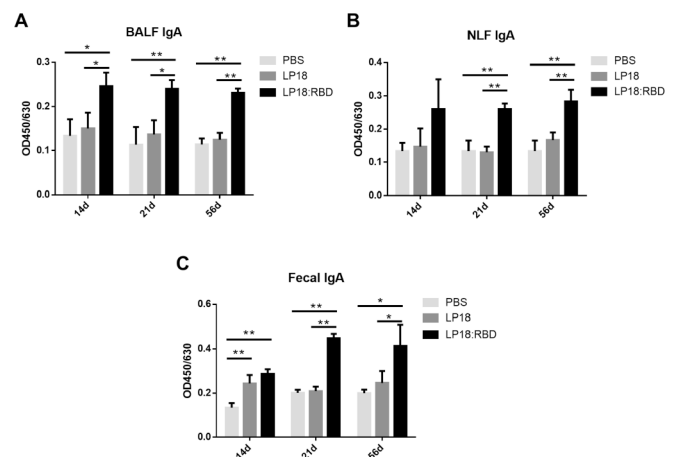


**Fig. 6.** The levels of antigen-specific IgA antibodies in the different mucosal sites. Antigen-specific IgA in the BALF (A), NLF (B), and fecal (C) samples of mice was detected by ELISA at 14, 21, and 56 days after primary immunization. Results are presented as mean ± SD of each group (\* $p < 0.05$ , \*\* $p < 0.01$ ).

increased, compared with the PBS or LP18 group via intranasal immunization from 14 days ( $p < 0.05$  or  $p < 0.01$ ), and reached a higher level after booster immunization until 56 days (Fig. 6C). These results indicated that antigen-specific IgA response was successfully elicited by the LP18:RBD via intranasal route in mice.

### 3.5. Activation of T cells induced by the LP18:RBD in mice

To investigate the effect of the LP18:RBD on cellular immunity responses in mice, the proportions of CD3 + CD4+ and CD3 + CD8+ T cells in splenic lymphocytes were analyzed at the 14, 21, and 56 days after prime immunization. As shown in Fig. 7A, the percentages of CD3 + CD4+ T cells in splenic lymphocytes of the LP18:RBD and LP18 groups were significantly higher than the PBS group at 56 days ( $p < 0.01$ ), and the LP18:RBD group maintained a higher level, compared with the PBS group throughout the time course. As shown in Fig. 7B, compared with the PBS group, the percentages of CD3 + CD8+ T cells in splenic lymphocytes of the LP18:RBD and LP18 groups were not increased significantly at 21 days after prime immunization, but those data showed significant increase at 56 days ( $p < 0.01$ ). The results as above indicated that the subtype differentiation of the CD3 + CD4+ T cells was increased by the LP18:RBD via intranasal route immunization in mice.

## 4. Discussion

*L. plantarum* is a potential carrier for vaccine delivery because of its beneficial characteristics of adhesion to mucosa [21] immunoregulation [22] antiviral property [23] and promoting intestinal barrier function [24]. Previous studies have shown that the expression system based on *L. plantarum* LP18 has been effective to display the viral heterologous protein [15,16]. However, the data about in vivo immunization are still lacking. In this study, we engineered *L. plantarum* for the surface expression of SARS-CoV-2 RBD protein and further demonstrated that it could induce immune responses effectively in mice.

In some elucidations about the vaccine of betacoronaviruses, the spike protein, and its RBD were regarded as the major target antigens for designing vaccines, and especially RBD was found to be an immunodominant and highly specific target of antibodies in SARS-CoV-2 patients [25]. It has been reported that several residues and compact conformation have changed in the SARS-CoV-2 RBD when compared with SARS-CoV, which led to that the SARS-CoV-2 RBD has stronger ACE2-binding affinity to the host cells [26]. Furthermore, research on recombinant vaccine targeting RBD showed better immunogenicity than other domains of spike protein, such as the extracellular domain protein (ECD), S1-subunit protein (S1), and S2-subunit protein (S2) [7]. A codon-optimized RBD sequence was therefore designed as target antigen in this study. Given the need for sufficient antigen for the mucosal vaccine to prime the immune system [9], the optimal conditions for the expression of the LP18:RBD were further explored, and the yield of the rRBD protein was measured. As a result, the amount of the rRBD protein in  $10^9$  CFU of LP18:RBD reached 3  $\mu$ g. This result was close to the report

of Kuczowska et al. in which 7  $\mu$ g of antigen protein was measured from  $10^9$  CFU of recombinant *L. plantarum* [19].

For enhancing the immunogenicity of the LP18:RBD, an endogenous signal peptide 1320 and DC-targeting peptide were linked to the N-terminus and C-terminus of the RBD protein respectively. The signal peptide 1320 was derived from the N-terminal lipoprotein from the analyses of the database LAB-Secretome [27], and it has been validated in assisting antigen protein anchor on the surface of the bacteria [15,16]. With the addition of the DC-targeting peptide, this strategy increased the chance to be recognized and presented by dendritic cells [28]. The results of fluorescence microscopy (Fig. 4B) and FCM (Fig. 4C) showed high reactivities between rRBD protein and anti-HA rabbit polyclonal antibody, which confirmed the surface localization of rRBD protein on the LP18:RBD. These results have been consistent with a previous study [16].

Following immunization, the LP18:RBD successfully elicited the IgA and T cell response via intranasal route immunization in mice. The IgA antibody located on mucous membranes plays a crucial role in mucosal immunity, it could neutralize pathogens, particularly in respiratory tract infections by the viruses like SARS-CoV, influenza virus, and respiratory syncytial virus (RSV), and protected the local mucosa from invading [29–31]. Recently, it has been demonstrated that the intranasal administration by adenovirus-vectored vaccine encoding spike protein (ChAd-SARS-CoV-2-S) induced robust IgA and neutralizing antibody responses and prevented SARS-CoV-2 infection to both upper and lower respiratory tract [32]. Similarly, in this work, increased specific IgA were detected in the nasal cavity, bronchus, and lung after intranasal administration of the LP18:RBD, which suggested that the humoral response could have been elicited by the LP18:RBD. Notably, the increased IgA was also detected in fecal samples, it is speculated that the gut-associated lymphatic tissue (GALT) could have been activated by intranasal administration of the LP18:RBD [33,34]. This result was consistent with previous experiments [35,36]. Moreover, the cell-mediated immune response reflected by the increased percentages of CD3 + CD4+ T cells in splenic lymphocytes was also elicited by intranasal administration of the LP18:RBD, which indicated that the differentiation of T cells leading to humoral immune responses may have been induced by LP18:RBD, meanwhile, similar results were also observed in mice via intranasal administration of *L. plantarum* LP18. Therefore, the beneficial immunomodulatory effect of *L. plantarum* might have been elicited in the study [22].

Generally, intranasal administration is considered as a primary route to initiate mucosal immune response as well as systemic immune response [34]. However, compared with other recombinant *L. plantarum* mucosal vaccines [19,20], it was disappointed that the specific IgG antibodies were not elicited in this work (Fig. S1). Some factors such as different vaccine formulation, route of administration, and schedule of immunization could lead to different types of immune response and antibodies generation [37]. Thus, to address this problem, the dosage and procedure of vaccination can be modified in further investigation. Overall, this study has taken a progressing step to develop a mucosal vaccine against SARS-CoV-2 using lactic acid bacterial delivery vector. Further, the study has provided a noninvasive immunization strategy. The next steps would focus on stimulating systemic immune response and challenge experiments using humanizing mice expressing human ACE2 or experimental primates.

## 5. Conclusion

In conclusion, a recombinant *L. plantarum* LP18:RBD expressing the RBD of SARS-CoV-2 was successfully constructed as a mucosal vaccine candidate. The rRBD protein was efficiently displayed on the surface of bacteria and revealed a good antigenicity. High expression of rRBD was obtained with the treatment of 200 ng/mL inducer at 33 °C for 6 h. The in vivo experiments demonstrated that antigen-specific immune responses were activated by intranasal immunization of the LP18:RBD.

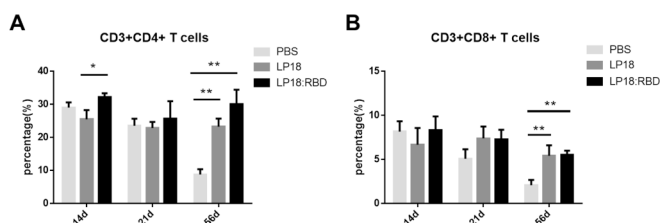


Fig. 7. The subset proportion of the T cells after intranasal administration of the LP18:RBD. The percentages of CD3 + CD4+ (A), and CD3 + CD8+ T cells (B) in the splenic lymphocytes of mice were detected by FCM at 14, 21, and 56 days after primary immunization. Results are presented as mean  $\pm$  SD of each group (\* $p < 0.05$ , \*\* $p < 0.01$ ).

This study suggested that *L. plantarum* is a potential vector for effectively delivering SARS-CoV-2 antigens to mucosal sites, which may serve as a new approach for the SARS-CoV-2 vaccine development.

Supplementary data to this article can be found online at <https://doi.org/10.1016/j.ijbiomac.2021.08.232>.

## Funding

This work was funded by the National Key Research and Development Program of China, China [No. 2017YFD0501002], the Changchun Science and Technology Bureau emergency project, China [No. 2020RW002], the National Natural Science Foundation of China, China [No. 31772747, 31802224], CAMS Innovation Fund for Medical Sciences, China [No. 2020-12M-5-001], and Basic Scientific Research Project of Wenzhou, China [No. S2020010].

## CRediT authorship contribution statement

Letian Li: methodology, validation, data curation, and writing original draft.

Maopeng Wang: methodology, formal analysis, writing original draft, and funding acquisition.

Jiayi Hao: methodology, validation, and writing original draft.

Jicheng Han: validation.

Tingting Fu: validation.

Jieying Bai: formal analysis.

Mingyao Tian: formal analysis and data curation.

Ningyi Jin: conceptualization and funding acquisition.

Guangze Zhu: conceptualization, writing-reviewing or editing, and supervision.

Chang Li: conceptualization, formal analysis, writing-reviewing or editing, funding acquisition, and supervision.

## Declaration of competing interest

The authors declare no conflicts of interest.

## References

- Q. Li, X. Guan, P. Wu, X. Wang, L. Zhou, Y. Tong, R. Ren, K.S.M. Leung, E.H.Y. Lau, J.Y. Wong, X. Xing, N. Xiang, Y. Wu, C. Li, Q. Chen, D. Li, T. Liu, J. Zhao, M. Liu, W. Tu, C. Chen, L. Jin, R. Yang, Q. Wang, S. Zhou, R. Wang, H. Liu, Y. Luo, Y. Liu, G. Shao, H. Li, Z. Tao, Y. Yang, Z. Deng, B. Liu, Z. Ma, Y. Zhang, G. Shi, T.T.Y. Lam, J.T. Wu, G.F. Gao, B.J. Cowling, B. Yang, G.M. Leung, Z. Feng, Early transmission dynamics in Wuhan, China, of novel coronavirus-infected pneumonia, *N. Engl. J. Med.* 382 (13) (2020) 1199–1207.
- D. Wrapp, N. Wang, K.S. Corbett, J.A. Goldsmith, C.L. Hsieh, O. Abiona, B. S. Graham, J.S. McLellan, Cryo-EM structure of the 2019-nCoV spike in the prefusion conformation, *Science* 367 (6483) (2020) 1260–1263.
- A.C. Walls, Y.J. Park, M.A. Tortorici, A. Wall, A.T. McGuire, D. Velesler, Structure, function, and antigenicity of the SARS-CoV-2 spike glycoprotein, *Cell* 181 (2) (2020) 281–292, e6.
- M. Yuan, N.C. Wu, X. Zhu, C.D. Lee, R.T.Y. So, H. Lv, C.K.P. Mok, I.A. Wilson, A highly conserved cryptic epitope in the receptor binding domains of SARS-CoV-2 and SARS-CoV, *Science* 368 (6491) (2020) 630–633.
- E.E. Walsh, R.W. Frencik Jr., A.R. Falsey, N. Kitchin, J. Absalon, A. Gurtman, S. Lockhart, K. Neuzil, M.J. Mulligan, R. Bailey, K.A. Swanson, P. Li, K. Koury, W. Kalina, D. Cooper, C. Fontes-Garfias, P.Y. Shi, O. Tureci, K.R. Tompkins, K. E. Lyke, V. Raabe, P.R. Dormitzer, K.U. Jansen, U. Sahin, W.C. Gruber, Safety and immunogenicity of two RNA-based Covid-19 vaccine candidates, *N. Engl. J. Med.* 383 (25) (2020) 2439–2450.
- Q. Gao, L. Bao, H. Mao, L. Wang, K. Xu, M. Yang, Y. Li, L. Zhu, N. Wang, Z. Lv, H. Gao, X. Ge, B. Kan, Y. Hu, J. Liu, F. Cai, D. Jiang, Y. Yin, C. Qin, J. Li, X. Gong, X. Lou, W. Shi, D. Wu, H. Zhang, L. Zhu, W. Deng, Y. Li, J. Lu, C. Li, X. Wang, W. Yin, Y. Zhang, C. Qin, Development of an inactivated vaccine candidate for SARS-CoV-2, *Science* 369 (6499) (2020) 77–81.
- J. Yang, W. Wang, Z. Chen, S. Lu, F. Yang, Z. Bi, L. Bao, F. Mo, X. Li, Y. Huang, W. Hong, Y. Yang, Y. Zhao, F. Ye, S. Lin, W. Deng, H. Chen, H. Lei, Z. Zhang, M. Luo, H. Gao, Y. Zheng, Y. Gong, X. Jiang, Y. Xu, Q. Lv, D. Li, M. Wang, F. Li, S. Wang, G. Wang, P. Yu, Y. Qu, L. Yang, H. Deng, A. Tong, J. Li, Z. Wang, J. Yang, G. Shen, Z. Zhao, Y. Li, J. Luo, H. Liu, W. Yu, M. Yang, J. Xu, J. Wang, H. Li, H. Wang, D. Kuang, P. Lin, Z. Hu, W. Guo, W. Cheng, Y. He, X. Song, C. Chen, Z. Xue, S. Yao, L. Chen, X. Ma, S. Chen, M. Gou, W. Huang, Y. Wang, C. Fan, Z. Tian, M. Shi, F.S. Wang, L. Dai, M. Wu, G. Li, G. Wang, Y. Peng, Z. Qian, C. Huang, J.Y. Lau, Z. Yang, Y. Wei, X. Cen, X. Peng, C. Qin, K. Zhang, G. Lu, X. Wei, A vaccine targeting the RBD of the S protein of SARS-CoV-2 induces protective immunity, *Nature* 586 (7830) (2020) 572–577.
- A. Haque, A.B. Pant, Efforts at COVID-19 vaccine development: challenges and successes, *Vaccines (Basel)* 8 (4) (2020) 739.
- N. Lycke, Recent progress in mucosal vaccine development: potential and limitations, *Nat. Rev. Immunol.* 12 (8) (2012) 592–605.
- K. Kuczkowska, C.R. Kleiveland, R. Minic, L.F. Moen, L. Overland, R. Tjaland, H. Carlsen, T. Lea, G. Mathiesen, V.G.H. Eijnsink, Immunogenic properties of lactobacillus plantarum producing surface-displayed mycobacterium tuberculosis antigens, *Appl. Environ. Microbiol.* 83 (2) (2017) (e02782-16).
- F. Bo, W.T. Yang, S.M. Shonyela, Y.B. Jin, K.Y. Huang, L.N. Shao, C. Wang, Y. Zhou, Q.Y. Li, Y.L. Jiang, H.B. Huang, C.W. Shi, J.Z. Wang, G. Wang, Y.H. Kang, G. L. Yang, C.F. Wang, Immune responses of mice inoculated with recombinant lactobacillus plantarum NCS expressing the fusion gene HA2 and 3M2e of the influenza virus and protection against different subtypes of influenza virus, *Virus Res.* 263 (2019) 64–72.
- R. Geriletu, H. Xu, M.A. Jia, X. Terkawi, H. Xuan, Zhang, immunogenicity of orally administered recombinant lactobacillus casei zhang expressing *Cryptosporidium parvum* surface adhesion protein P23 in mice, *Curr. Microbiol.* 62 (5) (2011) 1573–1580.
- S. Wang, N. Geng, D. Zhou, Y. Qu, M. Shi, Y. Xu, K. Liu, Y. Liu, J. Liu, Oral immunization of chickens with recombinant lactobacillus plantarum vaccine against early ALV-J infection, *Front. Immunol.* 10 (2019) 2299.
- E. Sorvig, G. Mathiesen, K. Naterstad, V.G.H. Eijnsink, L. Axelsson, High-level, inducible gene expression in lactobacillus sakei and lactobacillus plantarum using versatile expression vectors, *Microbiol. Sgm* 151 (2005) 2439–2449.
- M. Wang, S. Du, W. Xu, L. Song, P. Hao, N. Jin, L. Ren, C. Li, Construction and optimization of lactobacillus plantarum expression system expressing glycoprotein 5 of porcine reproductive and respiratory syndrome virus, *Int. J. Biol. Macromol.* 143 (2020) 112–117.
- M. Wang, T. Fu, J. Hao, L. Li, M. Tian, N. Jin, L. Ren, C. Li, A recombinant lactobacillus plantarum strain expressing the spike protein of SARS-CoV-2, *Int. J. Biol. Macromol.* 160 (2020) 736–740.
- T.J. Curiel, C. Morris, M. Brumlik, S.J. Landry, K. Finstad, A. Nelson, V. Joshi, C. Hawkins, X. Alarez, A. Lackner, M. Mohamadzadeh, Peptides identified through phage display direct immunogenic antigen to dendritic cells, *J. Immunol.* 172 (12) (2004) 7425–7431.
- V.G.H. Eijnsink, M.B. Brurberg, P.H. Middelhoven, I.F. Nes, Induction of bacteriocin production in lactobacillus sake by a secreted peptide, *J. Bacteriol.* 178 (8) (1996) 2232–2237.
- K. Kuczkowska, I. Myrbraten, L. Overland, V.G.H. Eijnsink, F. Follmann, G. Mathiesen, J. Dietrich, Lactobacillus plantarum producing a chlamydia trachomatis antigen induces a specific IgA response after mucosal booster immunization, *PLoS One* 12 (5) (2017), e0176401.
- M.L. Oliveira, A.P. Areas, I.B. Campos, V. Monedero, G. Perez-Martinez, E. N. Miyaji, L.C. Leite, K.A. Aires, P. Lee Ho, Induction of systemic and mucosal immune response and decrease in Streptococcus pneumoniae colonization by nasal inoculation of mice with recombinant lactic acid bacteria expressing pneumococcal surface antigen A, *Microbes Infect.* 8 (4) (2006) 1016–1024.
- N. Garcia-Gonzalez, R. Prete, N. Battista, A. Corsetti, Adhesion properties of food-associated lactobacillus plantarum strains on human intestinal epithelial cells and modulation of IL-8 release, *Front. Microbiol.* 9 (2018) 2392.
- D. Ren, C. Li, Y. Qin, R. Yin, S. Du, H. Liu, Y. Zhang, C. Wang, F. Rong, N. Jin, Evaluation of immunomodulatory activity of two potential probiotic lactobacillus strains by in vivo tests, *Anaerobe* 35 (Pt B) (2015) 22–27.
- I. Al Kassaa, D. Hober, M. Hamze, N.E. Chihib, D. Drider, Antiviral potential of lactic acid bacteria and their bacteriocins, probiotics antimicrob, *Proteins* 6 (3–4) (2014) 177–185.
- J. Wang, H. Ji, S. Wang, H. Liu, W. Zhang, D. Zhang, Y. Wang, Probiotic lactobacillus plantarum promotes intestinal barrier function by strengthening the epithelium and modulating gut microbiota, *Front. Microbiol.* 9 (2018) 1953.
- L. Du, Y. He, Y. Zhou, S. Liu, B.J. Zheng, S. Jiang, The spike protein of SARS-CoV-a target for vaccine and therapeutic development, *Nat. Rev. Microbiol.* 7 (3) (2009) 226–236.
- J. Shang, G. Ye, K. Shi, Y. Wan, C. Luo, H. Aihara, Q. Geng, A. Auerbach, F. Li, Structural basis of receptor recognition by SARS-CoV-2, *Nature* 581 (7807) (2020) 221–224.
- M. Zhou, D. Theunissen, M. Wels, R.J. Siezen, LAB-secretome: a genome-scale comparative analysis of the predicted extracellular and surface-associated proteins of lactic acid bacteria, *BMC Genomics* 11 (2010) 651.
- X. Hou, X. Jiang, Y. Jiang, L. Tang, Y. Xu, X. Qiao, L. Min, C. Wen, G. Ma, Y. Li, Oral immunization against PEDV with recombinant lactobacillus casei expressing dendritic cell-targeting peptide fusing COE protein of PEDV in piglets, *Viruses* 10 (3) (2018) 106.
- R. Mudgal, S. Nehul, S. Tomar, Prospects for mucosal vaccine: shutting the door on SARS-CoV-2, *Hum. Vaccin. Immunother.* 16 (12) (2020) 2921–2931.
- K.B. Renegar, P.A. Small Jr., L.G. Boykins, P.F. Wright, Role of IgA versus IgG in the control of influenza viral infection in the murine respiratory tract, *J. Immunol.* 173 (3) (2004) 1978–1986.
- R. Weltzin, V. Traina-Dorge, K. Soike, J.Y. Zhang, P. Mack, G. Soman, G. Drabik, T. P. Monath, Intranasal monoclonal IgA antibody to respiratory syncytial virus protects rhesus monkeys against upper and lower respiratory tract infection, *J. Infect. Dis.* 174 (2) (1996) 256–261.
- A.O. Hassan, N.M. Kafai, I.P. Dmitriev, J.M. Fox, B.K. Smith, I.B. Harvey, R. E. Chen, E.S. Winkler, A.W. Wessel, J.B. Case, E. Kashentseva, B.T. McCune, A.



- L. Bailey, H. Zhao, L.A. VanBlargan, Y.N. Dai, M. Ma, L.J. Adams, S. Shrihari, J. E. Danis, L.E. Gralinski, Y.J. Hou, A. Schafer, A.S. Kim, S.P. Keeler, D. Weiskopf, R. S. Baric, M.J. Holtzman, D.H. Fremont, D.T. Curiel, M.S. Diamond, A single-dose intranasal ChAd vaccine protects upper and lower respiratory tracts against SARS-CoV-2, *Cell* 183 (1) (2020) 169–184, e13.
- [33] J.R. McGhee, K. Fujihashi, Inside the mucosal immune system, *PLoS Biol.* 10 (9) (2012), e1001397.
- [34] H. Kiyono, S. Fukuyama, NALT- versus Peyer's-patch-mediated mucosal immunity, *Nat. Rev. Immunol.* 4 (9) (2004) 699–710.
- [35] A. Garcia-Diaz, P. Lopez-Andujar, J. Rodriguez Diaz, R. Montava, C. Torres Barcelo, J.M. Ribes, J. Buesa, Nasal immunization of mice with a rotavirus DNA vaccine that induces protective intestinal IgA antibodies, *Vaccine* 23 (4) (2004) 489–498.
- [36] E. Lorenzen, F. Follmann, S. Boje, K. Erneholt, A.W. Olsen, J.S. Agerholm, G. Jungersen, P. Andersen, Intramuscular priming and intranasal boosting induce strong genital immunity through secretory IgA in minipigs infected with chlamydia trachomatis, *Front. Immunol.* 6 (2015) 628.
- [37] H. Liu, H.P. Patil, J. de Vries-Idema, J. Wilschut, A. Huckriede, Evaluation of mucosal and systemic immune responses elicited by GPI-0100- adjuvanted influenza vaccine delivered by different immunization strategies, *PLoS One* 8 (7) (2013), e69649.